IOPscience iopscience.iop.org

Home Search Collections Journals About Contact us My IOPscience

A tunneling spectroscopy study of the pairing symmetry in the electron-doped $Pr_{1-x}LaCe_xCuO_{4-y}$

This article has been downloaded from IOPscience. Please scroll down to see the full text article.

2010 J. Phys.: Condens. Matter 22 045702

(http://iopscience.iop.org/0953-8984/22/4/045702)

View the table of contents for this issue, or go to the journal homepage for more

Download details:
IP Address: 129.252.86.83
The article was downloaded on 30/05/2010 at 06:39

Please note that terms and conditions apply.

J. Phys.: Condens. Matter **22** (2010) 045702 (7pp) doi:10.1088/0953-8984/22/4/045702

A tunneling spectroscopy study of the pairing symmetry in the electron-doped $Pr_{1-x}LaCe_xCuO_{4-y}$

F Giubileo[1], S Piano[2], A Scarfato[1], F Bobba[1], A Di Bartolomeo[1] and A M Cucolo[1]

[1] CNR-INFM Laboratorio Regionale SUPERMAT, and Dipartimento di Fisica 'E.R. Caianiello', Università di Salerno, Via S. Allende, 84081 Baronissi (SA), Italy
[2] School of Physics and Astronomy, University of Nottingham, Nottingham NG7 2RD, UK

E-mail: giubileo@sa.infn.it

Received 2 November 2009, in final form 11 December 2009
Published 12 January 2010
Online at stacks.iop.org/JPhysCM/22/045702

Abstract

We have performed scanning tunneling spectroscopy and point contact spectroscopy measurements on the electron-doped superconductor $Pr_{1-x}LaCe_xCuO_{4-y}$ ($x = 0.12$, $T_c \simeq 25$ K). We address the question of the symmetry of the order parameter and of the amplitude of the energy gap. We compare three possible scenarios, i.e. isotropic s-wave, 'anisotropic' s-wave, and d-wave. Evidence for a d-wave symmetry of the order parameter is given. From the temperature evolution of the dI/dV versus V characteristics we extract a BCS-like temperature dependence of the superconducting energy gap Δ. Despite the variety of measured spectra we give a consistent explanation for the whole set of data, indicating $\Delta = (3.6 \pm 0.2)$ meV and a ratio $2\Delta/K_BT_C \simeq 3.5 \pm 0.2$. In particular, point contact characteristics showing gap-like features at higher voltages have been interpreted by considering the formation of an intergrain Josephson junction in series with the point contact junction. Further confirmation of the correctness of the model is given by the behavior of the critical current of the intergrain Josephson junction versus temperature which follows the Ambegaokar–Baratoff behavior.

(Some figures in this article are in colour only in the electronic version)

1. Introduction

Since the discovery of high-T_C superconductivity (HTS) by Bednorz and Muller [1], a great number of experiments and theoretical studies have been performed to understand the mechanism responsible for the formation of the superconducting state. When the $d_{x^2-y^2}$ orbitals of the CuO_2 plane are half-filled, the system is an antiferromagnetic Mott insulator because of the strong on-site Coulomb repulsion between electrons [2]. The antiferromagnetic order is rapidly destroyed by hole doping the insulating CuO_2 planes, and the transition to the superconducting state takes place [2]. The discovery of the electron-doped cuprates clarified that not only holes but also electrons can dope the parent insulator favoring the formation of the superconducting state [3]. This fact had great influence on theories on the mechanism of HTS based on electron–hole symmetry [4–6]. In particular, there has been a large number of experiments studying the symmetry of the order parameter (OP) in cuprates, because this information is crucial for understanding the mechanism of this class of superconductors [7–9]. For the hole-doped cuprates, such as $La_{2-x}Sr_xCuO_4$ (LSCO), $YBa_2Cu_3O_7$ (YBCO), and $Bi_2Sr_2CaCu_2O_8$ (BSCCO), the general consensus is that they have a predominant d-wave pairing symmetry [10]. In contrast, there is no consensus concerning order parameter symmetry in electron-doped cuprates. While quasiparticle tunneling spectroscopy [11, 12] and earlier Raman spectroscopy [13] indicate an s-wave pairing in nearly optimally doped one-layer $Nd_{2-x}Ce_xCuO_4$ (NCCO) and $Pr_{2-x}Ce_xCuO_4$ (PCCO), tricrystal SQUID magnetometry [14], ARPES measurements [15, 16], and recent Raman spectroscopy results [17] are more consistent with a

 © 2010 IOP Publishing Ltd Printed in the UK

d-wave pairing. Recently, doping-dependent pairing symmetry has been inferred by point contact spectroscopy [18] and penetration depth measurements [19], where the change from d-wave pairing in the underdoped to s-wave in the optimally doped and overdoped one-layer PCCO is reported. Thus, the understanding of the origin and the nature of the pairing mechanism for HTS represents a formidable challenge for both theory and experiments, and one essential ingredient in the search for possible mechanisms of this phenomenon is the knowledge of the quasiparticle density of states (DOS), whose detailed shape and temperature dependence are constraining parameters to any theoretical model. From an experimental point of view, tunneling spectroscopy represents one of the fundamental tools to investigate the quasiparticle DOS near the Fermi energy (E_F) with high energy resolution ($\sim k_B T$) and phase-sensitive capability [20]. Indeed, differently from s-wave superconductors, in the d-wave case, the order parameter becomes zero along the nodes of a cylindrical Fermi surface, and changes sign in the orthogonal k directions. So, when an electron from a normal metal tunnels into a d-wave superconductor, the injected quasiparticle experiences a different pair potential depending on the angle α between the crystal orientation (e.g., a axis) of the superconductor and the interface [21, 22]. Due to the sign change of the OP, the quasiparticles at the interface form the so-called Andreev bound states (ABS), that can be probed as a zero bias conductance peak (ZBCP) in the tunnel conductance curve of a superconductor/insulator/normal metal junction, the amplitude of the ZBCP being dependent on the angle α.

In the literature two papers report the study of the conductance spectra on electron-doped PLCCO [23, 25]. In [23] the authors report scanning tunneling microscopy measurements on PLCCO, but they do not analyze the density of the states of the superconductor in terms of the investigation of the symmetry of the order parameter, in fact they concentrate their attention on revealing the bosonic energies. The other paper by Shan *et al* [25] presents the point contact Andreev reflection (PCAR) spectra obtained on the same material. They analyze the conductance spectra with a isotropic and anisotropic symmetry of the superconducting energy gap, and in the last case they affirm that their tunneling is along the antinodal direction. In any case they cannot distinguish between a s-wave or d-wave symmetry of the order parameter.

In this paper we report a tunneling spectroscopy study by means of scanning tunneling spectroscopy (STS) and point contact spectroscopy (PCS) techniques on the electron-doped cuprate $Pr_{1-x}LaCe_xCuO_{4-y}$. Different configurations from a tunneling regime to a contact regime have been investigated in the temperature range between 4.2 K and T_C in order to address the question of the symmetry of the superconducting OP.

High-quality single crystals of $Pr_{1-x}LaCe_xCuO_{4-y}$ were grown by the traveling-solvent floating-zone technique [24]. Superconducting samples have been obtained by annealing in pure Ar and we selected a sample with $x = 0.12$ corresponding to a bulk critical temperature $T_C \simeq 25$ K, as measured by ac susceptibility.

We model the conductance spectra by considering different symmetry of the order parameter: s-wave, d-wave and anisotropic s-wave. Analyzing the second derivative of I versus V we can exclude a s-wave symmetry of the order parameter. From the tunneling spectra it is difficult to distinguish between the other two symmetries, but from the PCAR spectra, that show a zero bias conductance peak, we have strong evidence of the d-wave symmetry of the order parameter.

2. STS experiment

The experiments were carried out by means of a UHV variable temperature (5–300 K) STM (Cryogenic-SFM from Omicron Nanotechnology). Scanning tunneling spectroscopy appears an excellent tool, with its high spatial and energy resolution allowing a direct measurement of the local quasiparticle density of states (LDOS) in a superconductor. In particular, the differential conductance obtained through STS can determine the superconducting energy gap with a resolution of few μeV. The tunneling junctions normal metal/insulator/superconductor (N/I/S) were achieved by mechanically approaching an etched Pt/Ir tip to the cleaved surface of the crystal. We performed voltage bias sweeps in the range ± 40 mV while measuring the tunneling current $I(V)$. The dynamical conductance curve $\mathrm{d}I/\mathrm{d}V(V)$ is then calculated by numerical derivative. Every spectra reported here is the result of 400 spectra continuously measured and then averaged in order to get noise reduction. In figure 1(a) we report an example of a tunneling conductance spectrum measured at low temperature ($T = 9$ K): we observe a single gap feature, with a slightly asymmetric shape, the peak height at the filled states being higher than that at the empty states. The origin of this asymmetry is still not clear [26], although it has often been observed in STS experiments on cuprates [27, 28]. The physical explanation of such an observation has been reported by several groups [29, 30].

Experimental conductance curves $\mathrm{d}I/\mathrm{d}V(V)$ are compared to the simulated curves obtained through Dynes' formula [31]:

$$\frac{\mathrm{d}I}{\mathrm{d}V}(V) \propto \int_{-\infty}^{+\infty} -\frac{\partial f(E-eV)}{\partial E}\,\mathrm{Re}\left[\frac{|E|-\mathrm{i}\Gamma}{\sqrt{(|E|-\mathrm{i}\Gamma)^2-\Delta^2}}\right]\mathrm{d}E \tag{1}$$

where f is the Fermi function and Γ is a phenomenological parameter that takes into account the finite lifetime of the quasiparticles.

We consider three different OP symmetries, namely:

isotropic s-*wave* ($\Delta(\vec{k}) = \Delta_0$) with constant amplitude of the OP in all directions in the k-space;

anisotropic s-*wave* ($\Delta(\vec{k}) = \Delta_0[\cos(k_x a) - \cos(k_y a)]^4 + \Delta_1$) where the OP has a constant phase but varying magnitude, with minimum value Δ_1;

$\mathrm{d}_{x^2-y^2}$-*wave* ($\Delta(\vec{k}) = \Delta_0[\cos(k_x a) - \cos(k_y a)]$), where Δ_0 is the maximum gap value and a is the in plane lattice constant. The gap is real and has strongly anisotropic magnitude with nodes and a phase reversal for orthogonal $\vec{k}$ directions.

The resulting numerical fits are very similar due to the effect of the temperature smearing and a significant Γ value

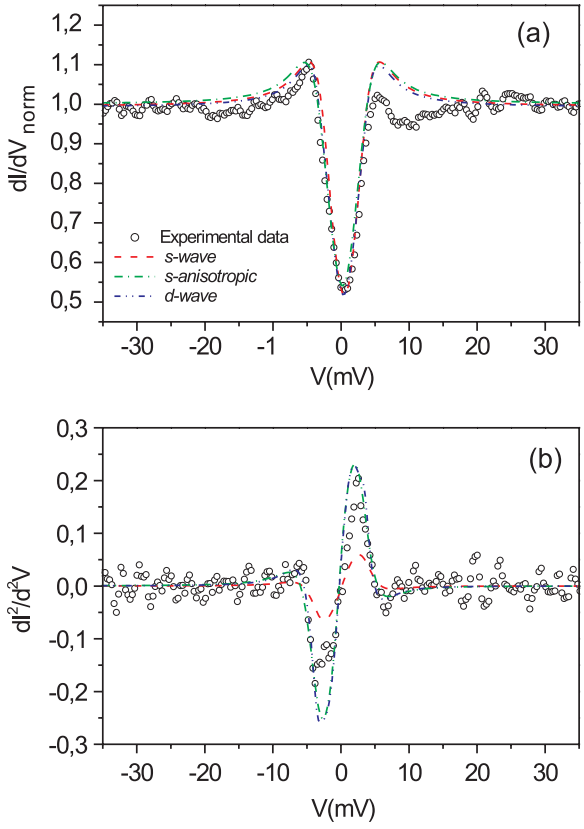

Figure 1. (a) Conductance spectrum at $T = 9$ K (black dots) and theoretical fitting for different symmetries of the order parameter: s-wave (red dashed line), s-anisotropic (green dash–dot line) and d-wave (blue dash–double dot line). (b) Comparison of the second derivatives.

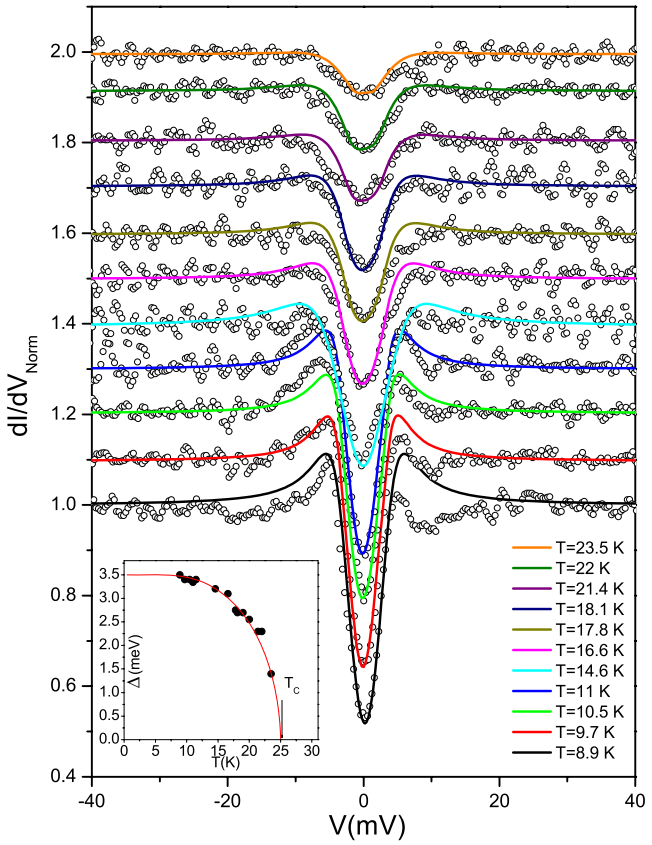

Figure 2. Temperature evolution of the conductance spectrum of figure 1(a). The solid lines are the theoretical fittings obtained by the tunneling model, using a d-wave symmetry of the order parameter. Inset: temperature dependence of the superconducting energy gap as inferred from the theoretical fittings. The solid (red) line is the BCS theoretical behavior.

that takes into account effects of physical origin (pair-breaking, inelastic scattering in the tunneling process, magnetic field) and those of experimental nature (temperature, bias jitter etc). The values of the fitting parameters are shown in table 1. The differences between the three simulated spectra reported in figure 1 are less significant than those with respect to the experimental data. Thus, we can refer to the second derivative $\mathrm{d}^2I/\mathrm{d}V^2$ that allows the enhancement of the discrepancies between the different curves. In figure 1(b), we observe that the isotropic s-wave hypothesis appears inappropriate to reproduce the experimental data. Although from the analysis of a single spectrum we cannot conclude anything about the pairing symmetry, we get a clear indication that in order to reproduce STS experimental data it is necessary to take into account an angular dependence of the OP in the k-space, thus excluding the possibility for conventional s-wave superconductivity in the $Pr_{1-x}LaCe_xCuO_{4-y}$ crystals.

By performing systematic measurements of the conductance spectra on a 1 μm^2 area, we found that the superconducting energy gap is highly homogeneous in its spatial distribution on a nanometer scale on the sample surface, showing a variation of the order of 5% of the gap amplitude.

In figure 2 we report the complete temperature dependence of the tunneling conductance spectra measured in the range between 9 and 25 K. The data are representative for several

Table 1. Fitting parameters used to model the conductance spectrum of figure 1 with different symmetries of the order parameter.

	Δ_0 (meV)	Δ_1 (meV)	Γ (meV)
s-wave	2.8	—	1.3
Anis. s-wave	2.4	0.9	1.6
d-wave	3.5	—	1.1

data sets measured in different locations. Experimental data (black empty dots in figure) are normalized, shifted for clarity and compared to theoretical fitting (solid lines) obtained by considering a d-wave symmetry of the OP. The numerical simulation has been performed by fixing the Γ parameter (temperature independent) to the value used for the fitting of the lowest temperature spectrum. In such a way, the energy gap Δ_0 remains the only free parameter used to reproduce the whole set of experimental data (the temperature being directly measured).

The resulting temperature behavior of the superconducting energy gap $\Delta_0(T)$, shown in the inset of figure 2, follows the BCS law, and gives confirmation of a local critical temperature $T_C \simeq 25$ K ($2\Delta/K_BT_C \simeq 3.3$), in agreement with the value from the bulk characterization of the material.

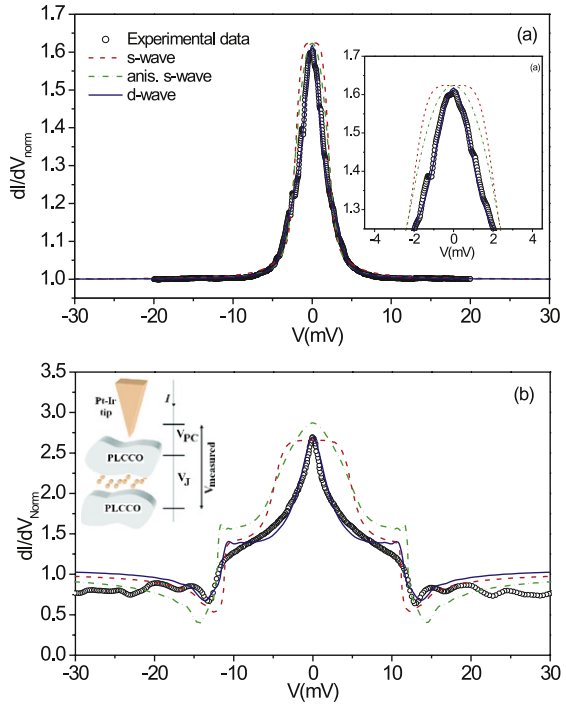

Figure 3. Normalized conductance spectra measured in the contact regime at low temperature ($T = 4.2$ K). (a) Experimental data are compared to the modified BTK model. (b) Example of conductance spectrum showing wider ZBCP. The theoretical fittings consider the real configuration of an intergrain Josephson junction in series to the point contact, as schematized in the inset.

3. Point contact experiment

The sample used for these experiments was shaped in very thin layers with the surface perpendicular to the *c*-axis crystal orientation, allowing a precise directional experiment in the STM configuration where the tip is separated from the sample and the charge carriers tunnel in the sample with k vectors in a very narrow angle cone around *c*-direction. In order to get discriminating information about the symmetry of the order parameter it is relevant to perform tunneling experiments in different directions, i.e. to measure conductance spectra where current contributions come from carriers having k vectors with a non-zero component in the *a*–*b* plane direction. Point contact spectroscopy (PCS) can be a suitable technique to get current contribution from different directions because the tip is pressed into the sample. Indeed, the PCS consists in establishing a contact between a tip of a normal metal and a superconducting sample (N–S junction). By varying the pressure of the tip on the sample it is possible to tune the junction from the tunneling regime (low transparent barrier) to the point contact regime (high transparent barrier). From a theoretical point of view, the N–S conductance spectra are described in the case of a BCS-type superconductor by Blonder, Tinkham and Klapwijk (BTK theory) [32], with the barrier between the normal metal and superconductor modeled by a delta function. The strength of the delta function is characterized by a dimensionless parameter Z. The $Z = 0$ limit signifies a completely transparent junction while $Z \gg 1$ corresponds to the tunneling regime. The BTK model has since been modified by Tanaka and Kashiwaya [33] for tunneling in superconductors with a d-wave symmetry of the order parameter, as follows:

$$\frac{\mathrm{d}I}{\mathrm{d}V}(V) = \frac{\int_{-\infty}^{+\infty} \mathrm{d}E \int_{-\frac{\pi}{2}}^{+\frac{\pi}{2}} \mathrm{d}\varphi\, \sigma(E,\varphi)\cos\varphi\left[-\frac{\mathrm{d}f(E+eV)}{\mathrm{d}(eV)}\right]}{\int_{-\infty}^{+\infty} \mathrm{d}E\left[-\frac{\mathrm{d}f(E+eV)}{\mathrm{d}(eV)}\right] \int_{-\frac{\pi}{2}}^{+\frac{\pi}{2}} \mathrm{d}\varphi\, \sigma_{\mathrm{N}}(\varphi)\cos(\varphi)}, \tag{2}$$

where

$$\sigma(E,\varphi) = \sigma_{\mathrm{N}}(\varphi)\frac{(1+\sigma_{\mathrm{N}}(\varphi))\Gamma_+^2 + (\sigma_{\mathrm{N}}(\varphi)-1)(\Gamma_+\Gamma_-)^2}{(1+(\sigma_{\mathrm{N}}(\varphi)-1)\Gamma_+\Gamma_-)^2},$$

$$\sigma_{\mathrm{N}}(\varphi) = \frac{1}{1+\tilde{Z}(\varphi)^2}, \qquad \tilde{Z}(\varphi) = Z\cos(\varphi),$$

$$\Gamma_\pm = \frac{E - \sqrt{E^2 - \Delta_\pm^2}}{\Delta_\pm}, \qquad \Delta_\pm = \Delta\cos[2(\alpha \mp \varphi)], \tag{3}$$

and where φ is the incident angle of the electrons at the N/S interface and α is the orientation angle between the a axis of the superconducting order parameter and the x axis.

3.1. Contact regime

In figure 3, as an example we show two normalized conductance spectra measured at low temperature ($T = 4.2$ K) by establishing different contacts on different areas of the same sample using as counter electrode a Pt–Ir tip. Both spectra are characterized by a well defined zero bias conductance peak (ZBCP) appearing with quite different shape, amplitude and energy width. The energy width of the ZBCP is lower than 10 meV in figure 3(a) while it appears wider, around 30 meV, in figure 3(b). At a first qualitative analysis, these data can appear quite puzzling and could be interpreted in terms of local, large variations of the superconducting energy gap. In the following, we will show that the numerical modeling allows the explanation all the experimental data giving a clear indication of a d-wave symmetry of the superconducting OP, with consistent values of the inferred amplitude of the energy gap. Both the spectra of figure 3 are compared to theoretical fittings taking into account the three possible symmetries. First of all, let us quantitatively analyze the curve of figure 3(a). The (blue) solid line in the figure represents the best fit resulting from the numerical simulation of experimental data by considering a d-wave symmetry of the OP in the modified BTK model [33].

A satisfactory agreement is obtained by using as fitting parameters the superconducting energy gap Δ, the barrier strength Z, the angle α and the phenomenological factor Γ. We notice that in the considered spectrum, both quasiparticle tunneling and Andreev reflection processes take place, since an intermediate Z value was necessary to simulate the barrier strength ($Z = 0.65$). Moreover, the angle α results to be about 0.45, indicating that the average transport current mainly flows along an intermediate direction between the nodal one $\alpha = \pi/4$ and that of the maximum amplitude of the energy gap $\alpha = 0$. Also reported in the figure are the fitting curves resulting from considering the s-wave and the anisotropic s-wave symmetry, evidencing a slight discrepancy

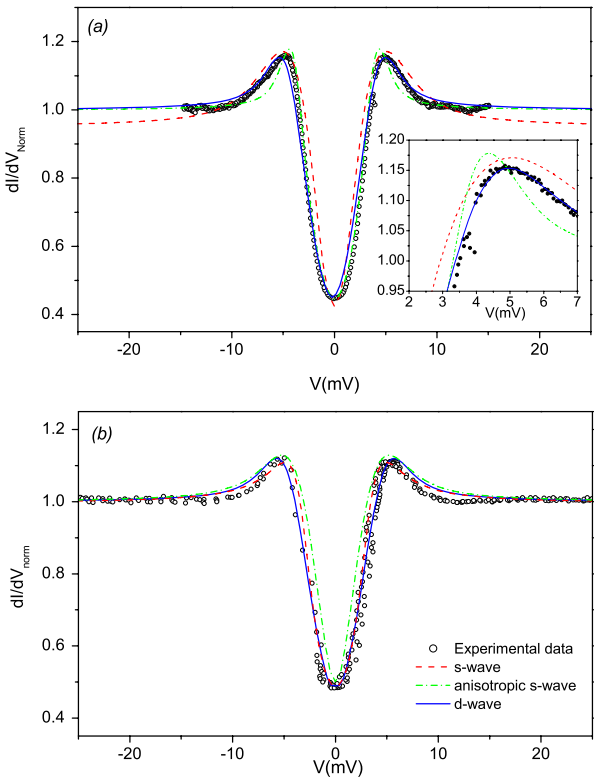

Figure 4. PCAR Conductance spectra at low T with the theoretical fit calculated by considering a Josephson junction in series: in this case the measured voltage corresponds to the sum of two terms $V_{\rm meas} = (I) = V_{\rm PC}(I) + V_{\rm J}(I)$, where $V_{\rm PC}$ and $V_{\rm J}$ are the voltage drops at the point contact junction and at the S/I/S intergrain Josephson junction, respectively.

in the modeling height and width of the ZBCP. We have found that the energy gap inferred from the theoretical (d-wave) fitting resulted to be $\Delta_0 = 3.6$ meV, in agreement with the value reported by the STS experiment.

We now address the analysis of the conductance spectrum with a wider ZBCP structure, reported in figure 3(b). This contact is the result of an increase of the pressure of the tip on the sample surface with respect to the case just discussed. The conductance characteristic also shows dip structures at higher energies which cannot be reproduced by using the BTK theory. The origin of these dips has been related to the formation of a junction in series, as already shown for $MgCNi_3$ [34], MgB_2 [35, 36], and Ru-based compounds [37, 38]. Then, to give a quantitative evaluation of the experimental data reported in figure 3(b), we need to consider a real configuration in which the Pt–Ir tip realizes a point contact junction on a PLCCO grain, which, in turn, is weakly coupled to another PLCCO grain, so forming a series of two junctions. The formation of such a series junction could be caused by the formation of a fracture in the sample structure just below the tip, due to the increase of the tip pressure. In this situation, the measured voltage is given by the sum of two terms: the voltage drop at the point contact $V_{\rm PC}$ and the one at the Josephson junction $V_{\rm J}$, so causing the observation of features at higher biases. According to this model, the conductance spectra can be calculated as

$$\sigma(V) = \frac{{\rm d}I}{{\rm d}V} = \left(\frac{{\rm d}V_{\rm PC}}{{\rm d}I} + \frac{{\rm d}V_j}{{\rm d}I}\right)^{-1}. \qquad (4)$$

Also in this case we have used different symmetries of the order parameter (s-wave, anisotropic s-wave and d-wave) to reproduce the experimental data. However, in this case, the structured ZBCP appearing in the conductance spectrum strongly indicates the presence of Andreev bound states due to the multiple Andreev reflections that take place at the N–S interface owing to a change of the sign of the OP. Therefore, as expected, only a d-wave symmetry can correctly reproduce such a feature, as is shown in figure 3(b). Moreover, from the theoretical model, we obtain a value of the superconducting energy gap $\Delta_0 = (3.6 \pm 0.1)$ meV, in agreement with the values extracted by the fitting of the PC spectrum in figure 3(a) and of the STS experiment in figure 2.

3.2. The tunneling regime

In this PCS experiment we also succeeded in realizing high-resistance contacts characterized by low transparency (the tunneling regime). In figure 4 we show two examples of conductance spectra measured in such a regime at $T = 4.2$ K, on the same sample but in two different locations.

High contact resistances were obtained by pushing the Pt–Ir tip into the PLCCO and then slightly releasing the pressure. In this case, the conductance curves show a typical quasiparticle tunneling shape, with a conductance minimum at zero bias and coherence peaks at voltages around ± 5 mV. From the theoretical fittings we found out that in order to reproduce the experimental data it is necessary to model the barrier strength by considering $Z = 2.6$ (in figure 4(a)) and $Z = 2.3$ (in figure 4(b)). As expected, we are dealing with a lower transparent barrier, approaching the tunneling regime with a still sensible contribution due to Andreev reflection processes. Once again, the only possibility to reproduce the experimental data is to take into account the contribution of an intergrain Josephson junction in series. The discrepancy among the different symmetries is clear in the inset of figure 4(a): we notice that the d-wave symmetry of the superconducting energy gap presents the best fit to the experimental data. We obtain a similar result with the spectrum of figure 4(b). We can extract from the experimental data an estimation of the energy gap amplitude $\Delta_0 = 3.5 \pm 0.1$ meV, matching the values obtained from the other measurements.

In table 2 we summarize the fitting parameters and the resulting values for the conductance spectra measured in the PCS experiments, by considering a d-wave symmetry of the order parameter.

3.3. Temperature dependencies

For almost all the contacts, we also performed the complete temperature dependence of the conductance characteristics in the temperature range between 4.2 and 30 K. As an example for the contact regime, we report in figure 5 the temperature evolution of the structured ZBCP of figure 3(b).

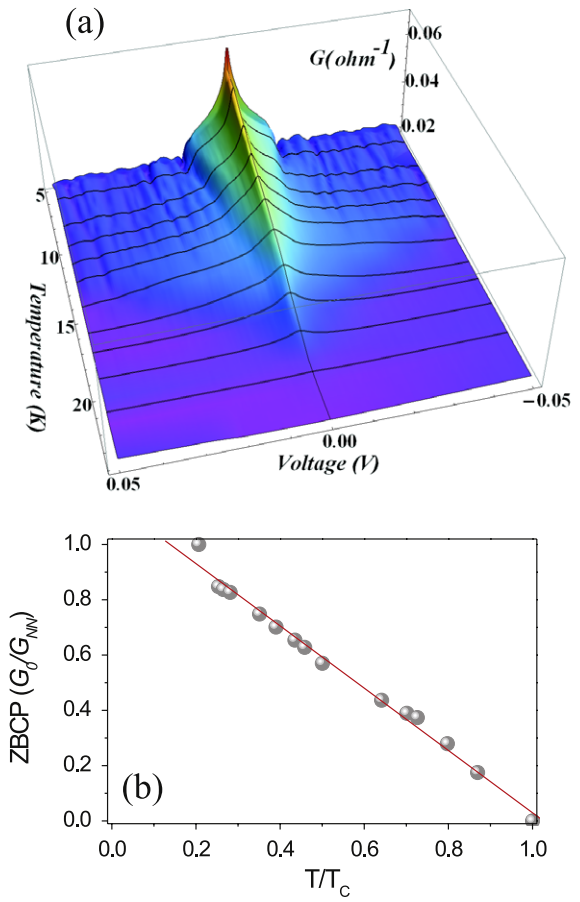

Figure 5. (a) Temperature dependence of the conductance spectra for the contact reported in figure 3(b). (b) Temperature evolution of the ZBCP amplitude.

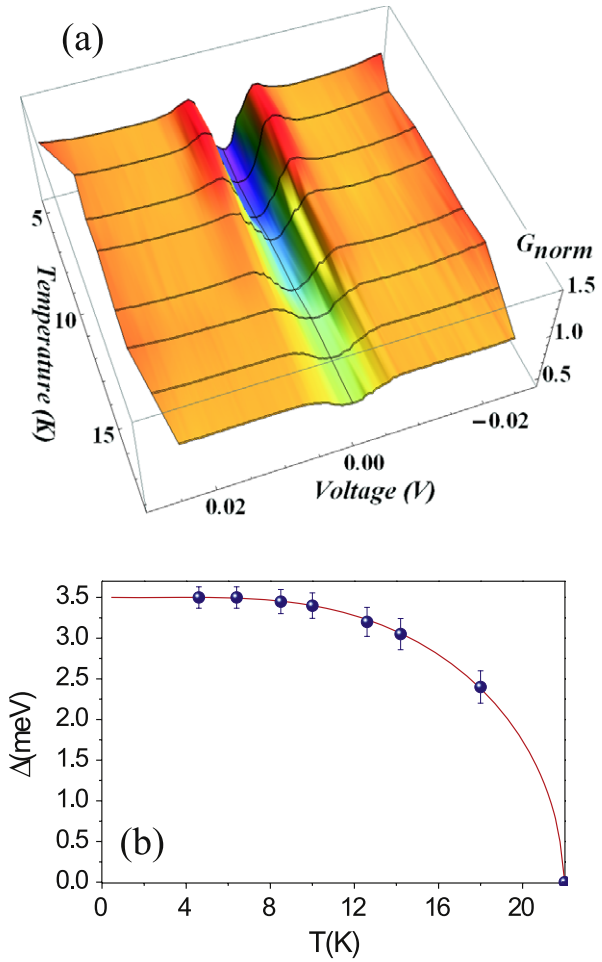

Figure 6. Temperature evolution of the conductance spectrum reported in figure 4(a). (b) Temperature dependence of the superconducting energy gap as extracted from the theoretical fittings.

Table 2. Fitting parameters used to model the low temperature conductance spectra of figures 3 and 4 considering the d-wave symmetry of the OP: energy gap Δ_0, orientation angle α, barrier strength Z, the smearing factor Γ, the resistance ratio between the two junctions in series R_J/R_{PC}, and the critical current I_J of the intergrain junction.

Data	Δ_0 (meV)	α	Z	Γ (meV)	R_J/R_{PC}	I_J (μA)
Figure 3(a)	3.6	0.45	0.65	0.5	No series	No series
Figure 3(b)	3.6	0.5	0.5	0	0.3	314
Figure 4(a)	3.5	0.33	2.6	0.8	0.3	2.4
Figure 4(b)	3.5	0.4	2.3	0.4	0.3	2.4

The amplitude of the peak is monotonously reducing on raising the temperature, until complete disappearance. This fact provides further evidence that the ZBCP is a consequence of the superconducting nature of PLCCO. By plotting, in figure 5(b), the peak amplitude versus temperature, we observe that the ZBCP amplitude decreases to zero at T_C in a linear way. The estimated local critical temperature of the superconducting PLCCO grain in contact with the Pt–Ir tip $T_C = 23$ K, is close to the bulk value and corresponds to a BCS ratio $2\Delta/K_BT_C \simeq 3.6$, that deviates less than 10% from the value resulting from the STS experiment of $2\Delta^{STS}/K_BT_C^{STS} \simeq 3.3$. We also report the temperature evolution of the conductance characteristics measured in the tunneling regime. In figure 6 we show the experimental data referring to the temperature evolution of the spectrum of figure 4(a). On raising the temperature, we observe a disappearance of the conductance coherence peaks and a simultaneous increase of the zero bias conductance. The measured spectrum for each temperature value has been theoretically fitted by considering the d-wave modified BTK model with the contribution of an intergrain Josephson junction in series. For all the curves, we fixed the strength of the barrier Z, the phenomenological parameter Γ, the angle α, and the ratio R_J/R_{PC} to the values obtained at the lowest temperature. In this way, the only free parameters to reproduce the experimental data were the energy gap Δ and the intergrain Josephson current I_J (the temperature being directly measured). The whole set of fitted curves allowed the extraction of the temperature dependence of the energy gap (reported in figure 6(b)) and of the current I_J (reported in figure 7). The energy gap shows a BCS-like behavior that evidences a local critical temperature $T_C \simeq 22$ K and corresponds to a BCS ratio $2\Delta/K_BT_C \simeq 3.7$. Moreover, the analysis of the temperature evolution, the intergrain Josephson current shown in figure 7, evidences that

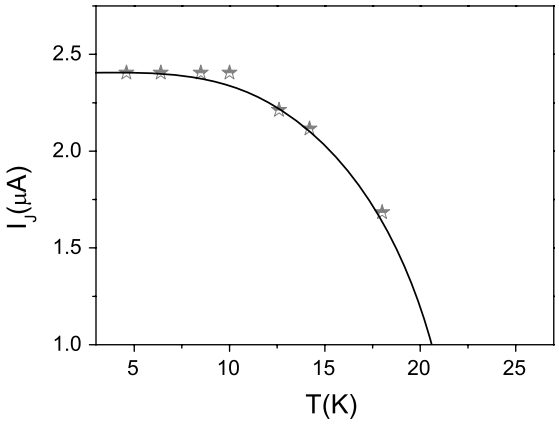

Figure 7. Critical current of the series Josephson junction versus temperature, as extracted from the theoretical fittings of the tunneling conductance spectra of figure 5(a).

I_J follows the Ambegaokar–Baratoff behavior correctly [39]. The experimental data reported in figure 7 are the values resulting from the theoretical fitting of each spectrum measured at different temperatures.

4. Conclusion

Tunneling spectroscopy was used to address the question of the symmetry of the order parameter in the superconducting $Pr_{1-x}LaCe_xCuO_{4-y}$ compound. Scanning tunneling spectroscopy and point contact spectroscopy experiments resulted in a huge variety of data, which we have analyzed by considering three possible symmetries for the OP: isotropic s-wave, 'anisotropic' s-wave, and d-wave. The theoretical simulation of the experimental data gives clear evidence of a d-wave symmetry. Moreover, despite the different features appearing in the tunneling conductance spectra, all data are consistent with a superconducting energy gap amplitude $\Delta \simeq 3.6 \pm 0.2$ meV, with a conventional BCS temperature dependence and a ratio $2\Delta/K_BT_C \simeq 3.5 \pm 0.2$. The correctness of the series Josephson junction model we have often used has been confirmed by the expected Ambegaokar–Baratoff dependence of the Josephson current extracted by the theoretical fittings.

References

[1] Bednorz J and Müller K A 1986 *Z. Phys.* B **64** 189
[2] Lee P A, Nagaosa N and Wen X-G 2006 *Rev. Mod. Phys.* **78** 17
[3] Tokura Y, Takagi H and Uchida S 1989 *Nature* **337** 345
[4] Anderson P W 1992 *Science* **256** 1526
[5] Dagotto E 1994 *Rev. Mod. Phys.* **66** 763
[6] Tsuei C C and Kirtley J R 2000 *Rev. Mod. Phys.* **72** 69
[7] Scalapino D J 1995 *Phys. Rep.* **250** 329
[8] Kirtley J R, Tsuei C C, Sun J Z, Chi C C, Yu-Jahnes L S, Gupta A, Rupp M and Ketchen M B 1995 *Nature* **373** 225
[9] Tsuei C C, Kirtley J R, Chi C C, Jahynes L-S Y, Gupta A, Shaw T M, Sun J Z and Ketchen M B 1994 *Phys. Rev. Lett.* **73** 593
[10] Van Harlingen D J 1995 *Rev. Mod. Phys.* **67** 515
[11] Alff L, Beck A, Gross R, Marx A, Kleefisch S, Bauch T, Sato H, Naito M and Koren G 1998 *Phys. Rev.* B **58** 11197
[12] Shan L, Huang Y, Gao H, Wang Y, Li S L, Dai P C, Zhou F, Xiong J W, Ti W X and Wen H H 2005 *Phys. Rev.* B **72** 144506
[13] Stadlober B, Krug G, Nemetschek R, Hackl R, Cobb J L and Markert J T 1995 *Phys. Rev. Lett.* **74** 4911
[14] Tsuei C C and Kirtley J R 2000 *Phys. Rev. Lett.* **85** 182
[15] Armitage N P *et al* 2001 *Phys. Rev. Lett.* **86** 1126
[16] Matsui H, Terashima K, Sato T, Takahashi T, Fujita M and Yamada K 2005 *Phys. Rev. Lett.* **95** 017003
[17] Blumberg1 G, Koitzsch A, Gozar A, Dennis B S, Kendziora C A, Fournier P and Greene R L 2002 *Phys. Rev. Lett.* **88** 107002
[18] Biswas A, Fournier P, Qazilbash M M, Smolyaninova V N, Balci1 H and Greene R L 2002 *Phys. Rev. Lett.* **88** 207004
[19] Skinta J A, Kim M-S, Lemberger T R, Greibe T and Naito M 2002 *Phys. Rev. Lett.* **88** 207005
[20] Wolf E L 1985 *Principles of Electron Tunneling Spectroscopy* (New York: Oxford University Press)
[21] Hu C R 1994 *Phys. Rev. Lett.* **72** 1526
[22] Lofwander T, Shumeiko V and Wendin G 2001 *Supercond. Sci. Technol.* **14** R53
[23] Niestemski F C, Kunwar S, Zhou S, Li S, Ding H, Wang Z and Dai P 2007 *Nature* **450** 1058
[24] Fujita M, Kubo T, Kuroshima S, Uefuji T, Kawashima K, Yamada K, Watanabe I and Nagamine K 2003 *Phys. Rev.* B **67** 014514
[25] Shan L, Huang Y, Wang Y L, Li S, Zhao J, Dai P, Zhang Y Z, Ren C and Wen H H 2008 *Phys. Rev.* B **77** 014526
[26] Das P, Koblischka M R, Wolf Th, Adelmann P and Hartmann U 2008 *Eur. Phys. Lett.* **84** 47004
[27] Sugita S, Watanabe T and Matsuda A 2000 *Phys. Rev.* B **62** 8715
[28] Pan S H, Hudson E W, Lang K M, Elsaki H, Uchida S and Davis J C 2000 *Nature* **403** 746
[29] Yusof Z, Zasadzinski J F, Coffey L and Miyakawa N 1998 *Phys. Rev.* B **58** 514
[30] Hirsch J E 1999 *Phys. Rev.* B **59** 11962
[31] Dynes R C, Narayanamurti V and Garno J P 1978 *Phys. Rev. Lett.* **41** 1509
[32] Blonder G E, Tinkham M and Klapwijk T M 1982 *Phys. Rev.* B **25** 4515
[33] Kashiwaya S and Tanaka Y 2000 *Rep. Prog. Phys.* **63** 1641
[34] Shan L, Tao H J, Gao H, Li Z Z, Ren Z A, Che G C and Wen H H 2003 *Phys. Rev.* B **68** 144510
[35] Giubileo F, Aprili M, Bobba F, Piano S, Scarfato A and Cucolo A M 2005 *Phys. Rev.* B **72** 174518
[36] Giubileo F, Bobba F, Scarfato A, Piano S, Aprili M and Cucolo A M 2007 *Physica* C **460–462** 587
[37] Piano S, Bobba F, Giubileo F, Cucolo A M, Gombos M and Vecchione A 2006 *Phys. Rev.* B **73** 064514
[38] Piano S, Bobba F, Giubileo F, Vecchione A and Cucolo A M 2006 *J. Phys. Chem. Solids* **67** 384
[39] Barone A and Paterno G 1981 *Physics and Applications of the Josephson Effect* (New York: Wiley)